Exploring the effects of Dasatinib, Quercetin, and Fisetin on DNA methylation clocks: a longitudinal study on senolytic interventions

Edwin Lee[1,*], Natàlia Carreras-Gallo[2,*], Leilani Lopez[2], Logan Turner[2], Aaron Lin[2], Tavis L. Mendez[2], Hannah Went[2], Alan Tomusiak[3], Eric Verdin[3], Michael Corley[4], Lishomwa Ndhlovu[4], Ryan Smith[2], Varun B. Dwaraka[2]

[1]Institute For Hormonal Balance, Orlando, FL 32819, USA
[2]TruDiagnostic, Lexington, KY 40503, United States
[3]Buck Institute for Research on Aging, Novato, CA 94945, USA
[4]Cornell University, Ithaca, NY 14853, USA
*Equal contribution

Correspondence to: Varun B. Dwaraka; **email:** varun@trudiagnostic.com

ABSTRACT

Senolytics, small molecules targeting cellular senescence, have emerged as potential therapeutics to enhance health span. However, their impact on epigenetic age remains unstudied. This study aimed to assess the effects of Dasatinib and Quercetin (DQ) senolytic treatment on DNA methylation (DNAm), epigenetic age, and immune cell subsets. In a Phase I pilot study, 19 participants received DQ for 6 months, with DNAm measured at baseline, 3 months, and 6 months. Significant increases in epigenetic age acceleration were observed in first-generation epigenetic clocks and mitotic clocks at 3 and 6 months, along with a notable decrease in telomere length. However, no significant differences were observed in second and third-generation clocks. Building upon these findings, a subsequent investigation evaluated the combination of DQ with Fisetin (DQF), a well-known antioxidant and antiaging senolytic molecule. After one year, 19 participants (including 10 from the initial study) received DQF for 6 months, with DNAm assessed at baseline and 6 months. Remarkably, the addition of Fisetin to the treatment resulted in non-significant increases in epigenetic age acceleration, suggesting a potential mitigating effect of Fisetin on the impact of DQ on epigenetic aging. Furthermore, our analyses unveiled notable differences in immune cell proportions between the DQ and DQF treatment groups, providing a biological basis for the divergent patterns observed in the evolution of epigenetic clocks. These findings warrant further research to validate and comprehensively understand the implications of these combined interventions.

INTRODUCTION

Senescence is defined as a stable growth arrest of cells that can limit the proliferation of damaged cells, which is important for tissue homeostasis [1, 2]. However, senescent cells also release harmful substances that can cause inflammation and damage to nearby healthy cells [2, 3]. Recent studies suggest that senescence may contribute to aging and age-related pathologies through the impossibility of tissue renewal by the stem cells caught in senescence or through the chronic inflammation of nearby cells that can lead to tissue dysfunction [4–6]. In fact, studies in mice have demonstrated that injecting senescent cells can induce age-related conditions like osteoarthritis, frailty, and reduced lifespan [7, 8].

Aging is characterized by gradual functional decline [9]. It is associated with increased risk of multiple

chronic diseases, geriatric syndromes, impaired physical resilience, and mortality [9–11]. For this reason, the pursuit of strategies to combat age-related diseases and promote healthy aging has increased in recent years.

Given the potential role of senescence in aging, senolytic drugs have emerged as promising candidates for extending lifespan. Some initially identified senolytics were Dasatinib, Quercetin, and Fisetin [12]. These molecules were drugs or natural products already used for other indications in humans, including anti-cancer therapies [13–15]. Dasatinib is a tyrosine kinase inhibitor approved by the FDA to treat myeloid leukemia [12, 16]. Quercetin is a flavonoid compound that induces apoptosis in senescent endothelial cells [12, 16]. Combined treatment with Dasatinib and Quercetin (DQ) has been demonstrated to decrease senescent cell burden in humans in multiple tissues [12, 17–20]; improve pulmonary and physical function along with survival in mice while lessening their age-dependent intervertebral disc degeneration [7, 21, 22]; and reduce senescence and inflammatory markers in non-human primates [23]. In human studies, patients with idiopathic pulmonary fibrosis, a senescence associated disease, improved 6-minute walk distance, walking speed, chair rise ability and short physical performance battery after 9 doses of oral DQ over 3 weeks [24]. Fisetin is another flavonoid compound that has gained recognition for its anti-proliferative, anti-inflammatory, and anti-metastatic properties [15, 25]. Fisetin has the potential to reduce senescence markers in multiple tissues in murine and human subjects [12, 26]. Administration of Fisetin to old mice restored tissue homeostasis, reduced age-related pathology, and extended median and maximum lifespan [26]. Notably, a comparative study has highlighted Fisetin as the safest and most potent natural senolytic among the tested compounds [26].

To date, research has not determined the effect of senolytics in biological aging measured by molecular biomarkers, such as the length of the telomeres, the proportion of immune cells, and the alteration of DNA Methylation. DNA methylation (DNAm) has emerged as a widely used biomarker for predicting health span and age-related diseases [27, 28]. In particular, multiple aging biomarkers, also known as clocks, have been developed since 2013. Among them, the first-generation clocks, such as the Hannum clock and Horvath clocks, utilize CpG sites that are highly associated with chronological age to estimate an individual's biological age [29, 30]. Second-generation clocks, including the DNAmPhenoAge and GrimAge, instead of being trained to predict chronological age, have been trained

to predict biological phenotypes, such as clinical features or proteins highly associated with aging. This new methodology led to higher hazard ratios of age-related outcomes for second-generation clocks compared to first-generation [31, 32]. Finally, in 2023, a third-generation clock was developed, the DunedinPACE, which measures the rate of aging rather than providing an overall age estimation [33].

Therefore, this study aims to comprehensively assess the impact of senolytic drugs on epigenetic aging through two longitudinal studies to address our research objective. The initial investigation focuses on a combination treatment of Dasatinib and Quercetin, while the subsequent phase incorporates Fisetin into the treatment regimen. The hypothesis of this prospective non-randomized clinical study posits that the combined administration of Quercetin and Dasatinib over 6 months will effectively decelerate participants' epigenetic biological aging, as measured at baseline, halfway point, and post-trial assessments. We anticipate that the synergy between Quercetin and Dasatinib will lead to a significant reduction in cell proliferation, thereby slowing the rate of aging and contributing to the improvement of the participants' overall epigenetic aging profile. This pilot study aims to establish the safety, efficacy, and feasibility of Quercetin and Dasatinib as a potential treatment to enhance the clinical care of healthy individuals, with the ultimate goal of extending longevity by mitigating the progression of epigenetic aging. The inclusion of Fisetin in the second treatment regimen had the aim of identifying differences in the effect of different senolytic drugs on epigenetic aging. This comprehensive approach will provide insights into how senolytic drugs influence epigenetic dynamics and contribute to our understanding of potential interventions in the process of senescence.

RESULTS

Figure 1 shows the design of the study. 28 individuals were enrolled in our cohort and split across two different studies. In the first study, a total of 19 participants underwent a 6-month treatment period with DQ, and blood samples were taken at baseline, 3 months, and 6 months. The age range of these individuals that were considered in the first study analyses were between 43.0 and 86.6 (Table 1). Following the completion of the initial treatment period, participants remained untreated for a duration of one year. Out of the initial group, 10 participants continued in the trial, while 9 new participants joined the study, which resulted in a total sample size of 19. In the second trial, all participants underwent a 6-month treatment with DQ and Fisetin, with measurements

taken at baseline and 6 months. The average age of the participants in these two studies was 60.9, ranging from 44.5 to 88.0. The percentage of male participants varied across the studies: 57.9% in the DQ study and 42.1% in the DQF study.

Impact of senolytic drugs on epigenetic age

To investigate the impact of the combination of DQ and the combination of DQF on epigenetic age, we assessed biological age using the principal component versions of multiple epigenetic clocks: the first-generation Horvath pan tissue clock, the Horvath skin and blood clock, and the Hannum clock; the second generation DNAmPhenoAge and GrimAge; and third generation DunedinPACE. For these clocks except DunedinPACE, we calculated the epigenetic age acceleration (EAA) after adjusting the values by age and principal components.

We observed that PC Horvath pan tissue EAA significantly increased after 3 months of DQ treatment (p-value=$6.7 \cdot 10^{-06}$). However, this increase was followed by a decrease 3 months later (p-value=$2.6 \cdot 10^{-4}$), resulting in non-significant differences between the baseline and the 6-month time point (p-value=0.23) (Figure 2A and Table 2). Besides, we detected a significant increase in this clock after 6 months of DQF treatment (p-value=0.017, see Table 3).

Regarding the other first-generation clocks, PC Horvath Skin and Blood EAA and PC Hannum EAA, we identified a significant increase following DQ treatment, particularly at the 3-month period (Figure 2B, 2C and Table 2). However, we did not observe significant changes in EAA after DQF treatment for these clocks (Table 3).

For second-generation clocks, we observed a significant increase between baseline and 3-month tests after DQ treatment in PC DNAmPhenoAge (p-value=0.005) and between baseline and 6-month test (p-value=0.038). On the other hand, PC GrimAge and the third-generation clock, DunedinPACE, remained stable after the treatment. For DQF treatment, all the second and third-generation clocks were unchanged. We have also assessed differences using a one-way ANOVA analysis and identified that a significance of 0.05 was not achieved, suggesting a congruence with the t-test results.
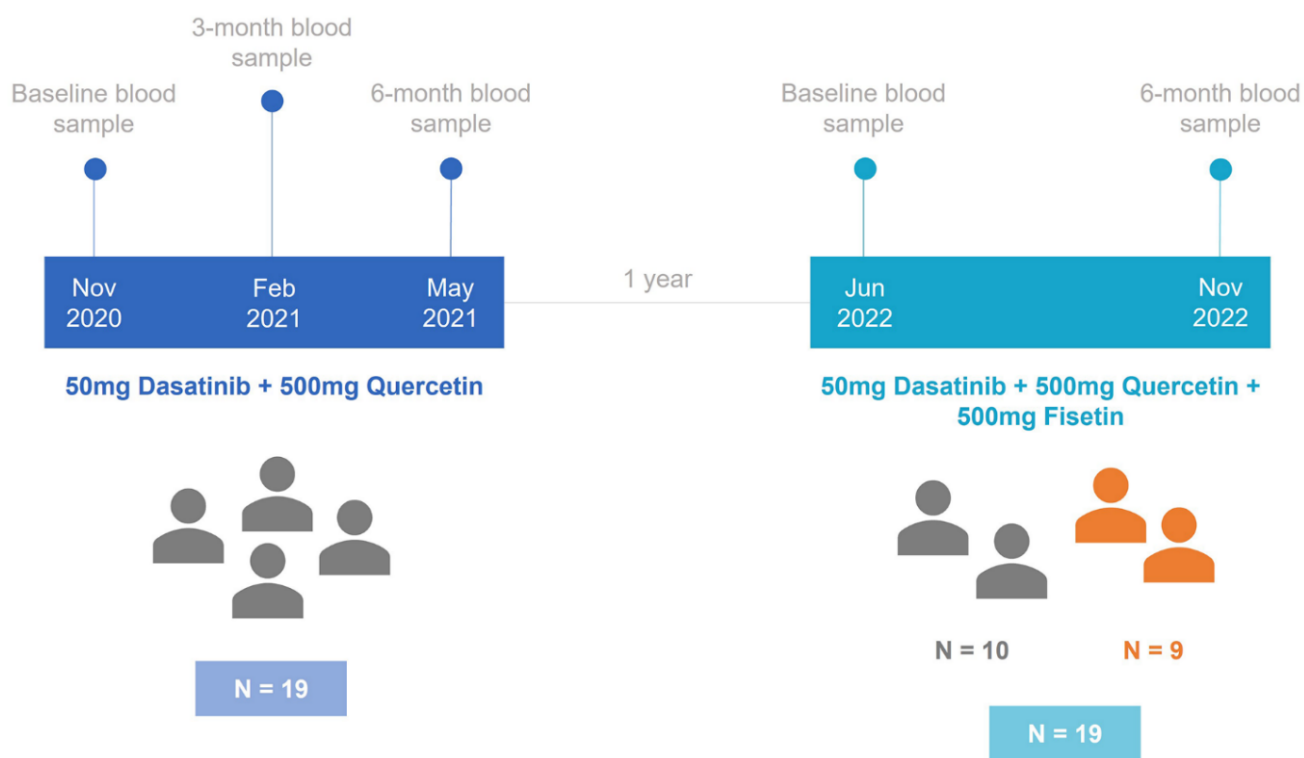
Figure 1. Timeline diagram for the study design. In the first study, 19 individuals were treated with 50mg of Dasatinib and 500mg of Quercetin. After one year, the second study started with 10 participants from the first study and 9 new participants. These individuals were treated with 50mg of Dasatinib, 500mg of Quercetin, and 500mg of Fisetin.

Table 1. Characteristics of participants in both trials.

	Dasatinib and Quercetin study (study 1)	Dasatinib, Quercetin, and Fisetin study (study 2)
Sample Size	19 (New = 19)	19 (New = 9, Continued = 10)
Age in years, mean (range)	59.6 (43.0 - 86.6)	60.9 (44.5 - 88.0)
Sex, male	11 (57.9%)	8 (42.1%)

We also evaluated the changes observed by the recently developed IntrinClock, as it is agnostic to immune cell changes that have been shown to influence the reliable quantification of epigenetic age [34]. However, no significant differences were observed in any of the trials.

Impact of senolytic drugs on DNAm telomere length and mitotic clock epigenetic methylation prediction algorithms

Cells with critically short telomere lengths are also known to undergo senescence once they approach their Hayflick limit [35], therefore we investigated the potential changes due to telomere length using the DNAm predictor for telomere length (DNAmTL) [36]. We found significant alterations in the DQ group, but not in the DQF group. Specifically, we observed a significant decrease in PC DNAm telomere length after the whole treatment (p-value=0.01, see Figure 3A), which was even more significant after adjusting by age (p-value=$4.4\cdot10^{-4}$, see Figure 3B). Importantly, the difference in telomere length acceleration between baseline and 3 months was larger and more significant (p-value=$7.5\cdot10^{-5}$) than the difference between baseline and 6 months (p-value=$4.4\cdot10^{-4}$).

Mitotic clock metrics were also employed to evaluate relative changes in stem cell replication. At the 3-month mark of DQ treatment, we observed a decrease in both the total number of stem cell divisions and the intrinsic tissue stem cell divisions, although these changes were not statistically significant (p-value=0.22 and p-value=0.22, respectively, see Figure 4). However, between 3-month and 6-month points, a significant increase was evident in both mitotic clocks (p-value=$2.4\cdot10^{-4}$ and p-value= $7.8\cdot10^{-4}$, respectively). In the case of DQF treatment, no significant differences were found between the baseline and the 6-month measurement.

Impact of senolytic drugs on whole blood immune cell composition

We utilized EpiDISH (2023) to quantify 12 different immune cell subsets and assess changes within these subsets. During the 6-month period of DQ treatment, significant alterations were observed in CD4T Naive cells, B Naive cells, and monocytes (Table 4). The most notable and significant change was in CD4T Naive Cells, which exhibited a slight decrease at the 3-month mark (p-value=0.628) and experienced a
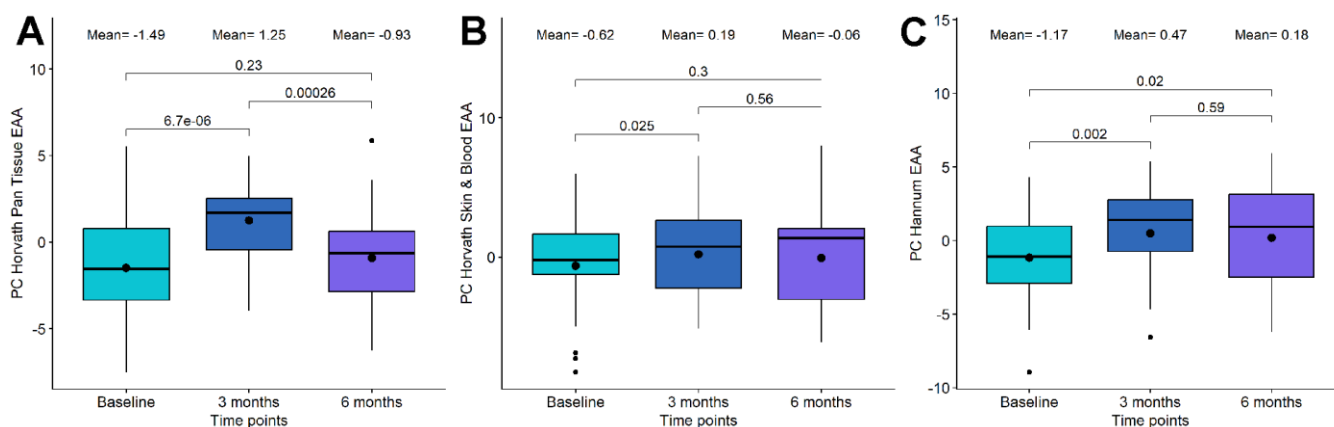
Figure 2. Boxplot showing the evolution of epigenetic age acceleration (EAA) first-generation clocks in the Dasatinib and Quercetin (DQ) study. (**A**) PC Horvath pan tissue EAA. (**B**) PC Horvath Skin and Blood EAA. (**C**) PC Hannum EAA. In the X-axis, the time points of measurements, in the Y axis, the EAA measure. On the top, the mean values at each time point and the p-values of the paired t-tests. The box represents the interquartile range (IQR) with the median represented as a horizontal line and the mean as the dot. The vertical lines show the minimum and maximum values. When outliers are identified, those values are represented as dots.

Table 2. Statistical analysis for comparing baseline, 3 months, and 6 months epigenetic age acceleration (EAA) in the Dasatinib and Quercetin study.

	Mean			Baseline vs 3-month		Baseline vs 6-month		3-month vs 6-month	
	Base	3m	6m	T-score	P-value	T-score	P-value	T-score	P-value
PC Horvath pan tissue EAA	-1.485	1.254	-0.926	-6.258	**$6.7 \cdot 10^{-6}$**	-1.230	0.234	4.527	**$2.6 \cdot 10^{-4}$**
PC Horvath Skin and Blood EAA	-0.625	0.194	-0.064	-2.450	**0.025**	-1.075	0.297	0.598	0.557
PC Hannum EAA	-1.165	0.474	0.184	-3.622	**0.002**	-2.561	0.020	0.546	0.592
PC GrimAge EAA	-0.173	-0.179	0.374	0.016	0.988	-1.431	0.170	-1.476	0.157
PC DNAm Pheno Age EAA	-1.766	0.891	0.134	-3.237	**0.005**	-2.240	0.038	0.936	0.362
PC DNAmTL EAA	0.043	-0.024	-0.010	5.098	**$7.5 \cdot 10^{-5}$**	4.286	$4.4 \cdot 10^{-4}$	-0.931	0.364
DunedinPACE	0.929	0.923	0.927	0.392	0.699	0.112	0.912	-0.230	0.821
Intrinclock EAA	0.039	-0.428	0.389	0.714	0.484	-0.499	0.624	-1.235	0.233

The first three columns show the mean values for each EAA clock at each time point. The next columns have information about the t-test between baseline and 3-month test, between baseline and 6-month test, and between 3-month and 6-month tests, respectively. In bold, the significant associations are highlighted.

Table 3. Statistical analysis for comparing baseline and 6-month epigenetic age acceleration (EAA) in the Dasatinib, Quercetin, and Fisetin study.

	Mean		Baseline vs 6-month	
	Baseline	6-month	T-score	P-value
PC Horvath pan tissue EAA	-0.201	1.607	-2.643	**0.017**
PC Horvath Skin and Blood EAA	-0.057	0.826	-1.838	0.083
PC Hannum EAA	-0.162	0.853	-1.774	0.093
PC GrimAge EAA	0.101	0.057	0.140	0.890
PC DNAmPhenoAge EAA	-0.033	0.964	-1.094	0.288
PC DNAmTL EAA	0.005	-0.027	1.698	0.107
DunedinPACE	0.937	0.918	1.016	0.323
Intrinclock EAA	0.637	-0.637	1.608	0.125

The first two columns show the mean values for each EAA clock at each time point. The next columns have information about the t-test between baseline and 6-month test. In bold, the significant associations are highlighted.

more substantial decline between the 3 and the 6-month marks (p-value=0.029). B Naive cells displayed an insignificant increase for the global treatment (p-value=0.059), but we observed a significant increase between 3 and 6 months (p-value=0.001). Monocytes showed a global increase after 6 months of treatment (p-value=0.003) that was characterized by a significant decrease at 3 months (p-value=0.035) followed by a significant increase between 3 and 6 months (p-value=$3.0 \cdot 10^{-5}$). Conversely, CD4T Memory, CD8T Naive, CD8T Memory, B Memory, basophil, regulatory T cells, eosinophil, Natural Killer, and Neutrophil did not exhibit significant changes.

Regarding the impact of DQF on immune cells, B Naive cells (Bnv) demonstrated a significant decrease after 6 months (p-value=$3.0 \cdot 10^{-4}$), which contrasts with the observations from DQ treatment. No significant changes were observed in the proportions of other immune cell subsets (Table 5).

Since most of the epigenetic clocks, especially the first-generation clocks, are dependent on immune subsets, we calculated the correlation between the EAA metrics and the immune cells proportions. As expected, we did not observe significant correlations between IntrinClock and immune cells. However, we observed high correlations between the other clocks and most of the

immune cells (Figure 5). Thus, we decided to calculate immune EAA adjusting EAA values by all the immune cells that were significantly associated to the clocks (CD4T naive and memory cells, B naive and memory cells, CD8T naive and memory cells, natural killers, and neutrophils) and see whether the trends in first-generation clocks after DQ treatment were maintained. We found that the significance and direction of the associations were not modified after adjusting by immune cells, indicating that the increase of epigenetic age after DQ treatment was not due to the alteration of immune cell subsets (Supplementary Figure 1).

## Impact of senolytic drugs on whole-genome DNA methylation

We also assessed global modification of DNAm in those individuals who were treated with DQ and those with DQF. To this end, we performed an Epigenome-Wide Association Study (EWAS) comparing the methylation levels for all the CpG sites in the genome at different timepoints in each trial (Supplementary Table 1).

The first EWAS was performed between baseline and 3 months of DQ treatment. In this case, we identified 11 CpG sites differentially methylated, 4 of them hypermethylated and 7 hypomethylated after 3 months. These probes were mapped to 8 genes. Among them, *TGIF1, SORBS2,* and *ZNF768* were implicated in senescence [37–39]. Using a less restrictive threshold of p-value lower than $1 \cdot 10^{-4}$, we performed an enrichment analysis. Among the 305 probes identified, we found three enriched processes highly related with senescence, such as glycolic process, vesicle recycling and endocytosis, and cytoskeletal organization [40–42].

Second, we evaluated the differences in global methylation between baseline and 6 months after DQ treatment. In this case, we only saw 2 CpG sites differentially methylated with an adjusted p-value lower than 0.05. One of them was hypermethylated and the other hypomethylated after a period of 6 months. The GREAT analysis was performed with the 475 CpG sites with a nominal p-value lower than $1 \cdot 10^{-4}$. Although multiple gene ontology terms were identified as enriched, none of them were directly associated with aging or senescence.

Finally, when we compared the methylation levels between baseline and 6 months after DQF treatment, we identified 208 significant probes. Among them, approximately 50% were hypomethylated and 50% were hypermethylated. The GREAT analysis was
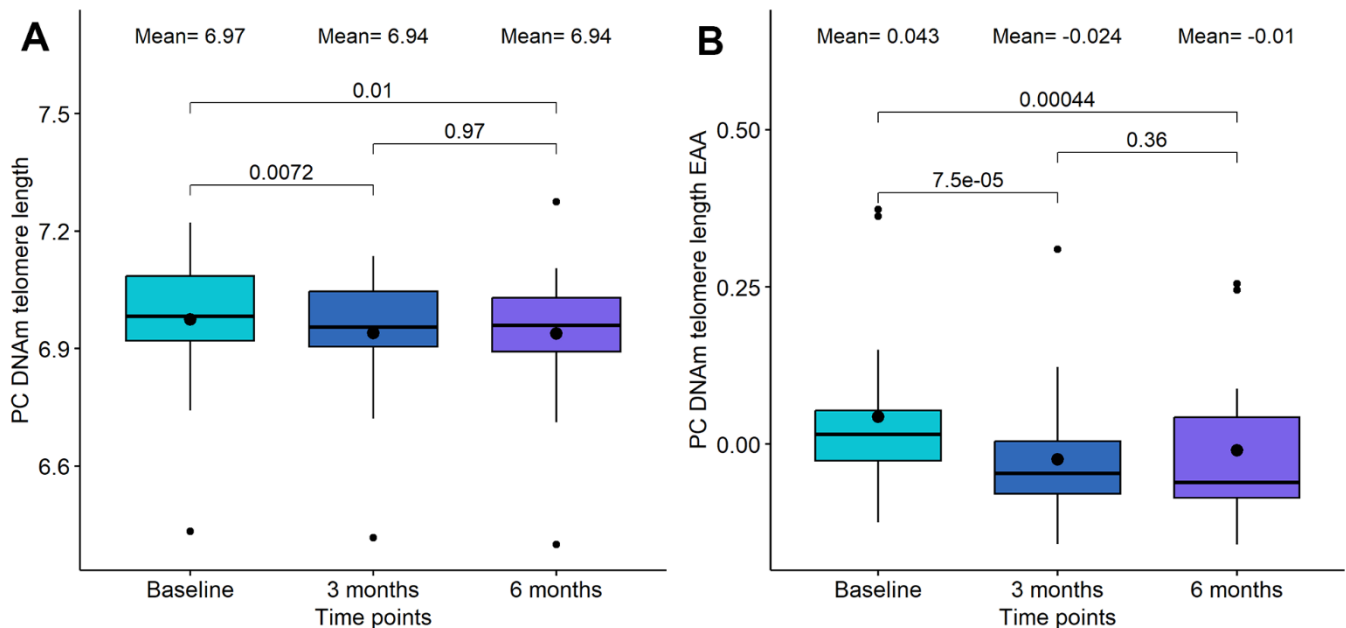
Figure 3. Boxplot showing the evolution of DNA methylation (DNAm) based telomere length in the DQ study. (**A**) DNAm telomere length. (**B**) DNAm telomere length acceleration. In the X-axis, the time points of measurements, in the Y axis, the epigenetic metric. On the top, the mean values at each time point and the p-values of the paired t-tests. The box represents the interquartile range (IQR) with the median represented as a horizontal line and the mean as the dot. The vertical lines show the minimum and maximum values. When outliers are identified, those values are represented as dots.

performed using 556 probes with a p-value below $1 \cdot 10^{-4}$ and revealed multiple enriched pathways associated with senescence, such as epithelial cell proliferation, platelet dense granule membrane, cell junction, and positive regulation of cardiac muscle cell apoptotic process [43–47].

Clinical and DNAm proteomic surrogate analysis

The major hypothesized mechanism for the negative impacts of senescence is through the increased senescence-associated secretory phenotypes (SASP) which lead to high inflammatory cytokine signaling from senescent cells in a paracrine fashion. As an alternative to robust clinical lab measurements of inflammatory mediators, we used methylation risk scores surrogates to predict and quantify predicted changes in circulating proteomic markers [48]. The quantification of these markers and the comparison between the different timepoints are included in Supplementary Tables 2, 3.

We paid special attention to inflammation and inflammatory proteomic EpiScore analysis and these are listed in Table 6. In this analysis, we see some increased inflammatory mediators at 3 months which decrease from the 3 to 6-month timepoints. These inflammatory-associated proteins include CRP, CXCL9, CXCL11,

CCL17, and TGF-alpha. We see opposite trends with other inflammation-associated markers such as Complement C4 and Complement C5a. Many inflammatory mediators for the innate adaptive immune system were not registered as significant in this analysis.

DISCUSSION

In the context of our study, the administration of senolytic drugs Dasatinib and Quercitin significantly increases biological age measured by first generation clocks, with DNAmPhenoAge being the only second-generation clock showing an increase. Notably, there is a lack of significant changes in second and third-generation clocks such as GrimAge and DunedinPACE, and no noteworthy alterations are observed with the addition of Fisetin to the protocol. The unique trend in the increase in DNAmPhenoAge, distinct from the other phenotypically trained clocks, is explicable considering its characterization as a hybrid between first and second-generation clocks. Unlike GrimAge and DunedinPoAm, the variable used for training DNAmPhenoAge includes chronological age, mirroring its derivation that adjusts for chronological age effects. This similarity is further elucidated by its module composition, reflecting similarity to first-generation trained chronological clocks [49].
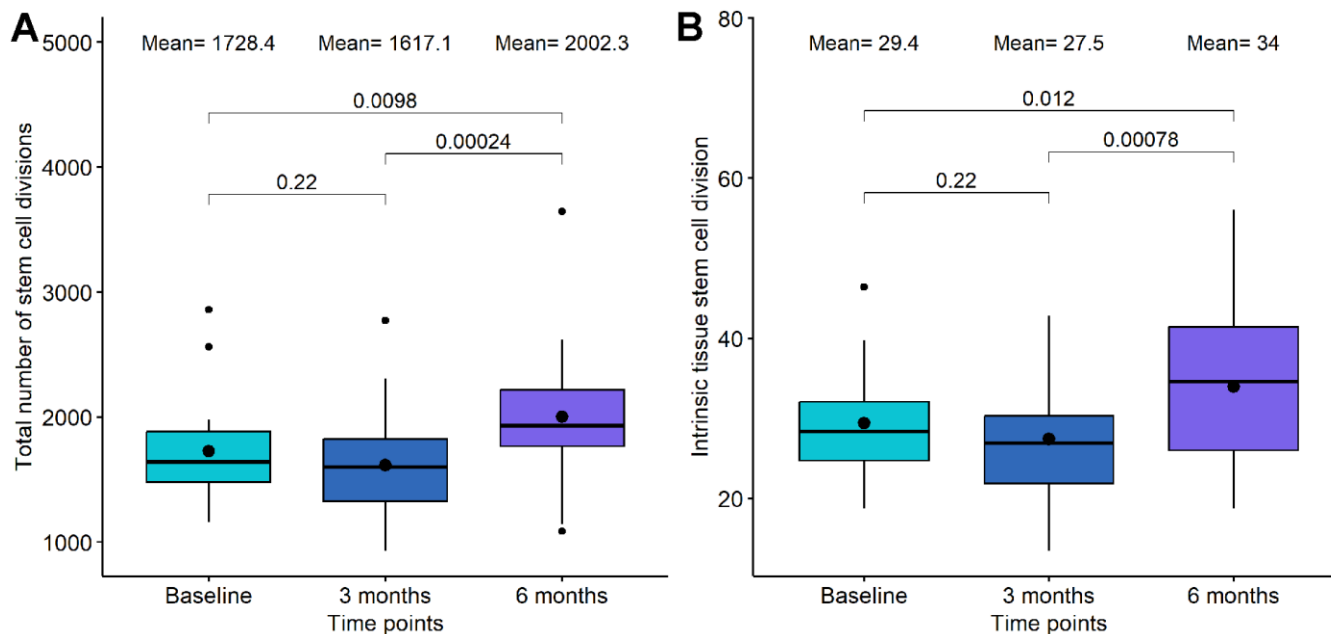
Figure 4. Boxplot showing the evolution of mitotic clocks in the Dasatinib and Quercetin study. (**A**) Total number of stem cell divisions. (**B**) Intrinsic tissue stem cell division. In the X-axis, the time points of measurements, in the Y axis, the number of divisions. On the top, the mean values at each time point and the p-values of the paired t-tests. The box represents the interquartile range (IQR) with the median represented as a horizontal line and the mean as the dot. The vertical lines show the minimum and maximum values. When outliers are identified, those values are represented as dots.

Table 4. Statistical analysis for comparing baseline, 3 months, and 6 months immune cell proportions in the Dasatinib and Quercetin study.

	Mean			Baseline vs 3-month		Baseline vs 6-month		3-month vs 6-month	
	Base	3m	6m	T-score	P-value	T-score	P-value	T-score	P-value
CD4T naive cells	0.077	0.074	0.060	0.493	0.628	2.228	**0.039**	2.364	**0.029**
Basophiles	0.020	0.021	0.020	-1.147	0.266	-0.408	0.688	0.439	0.666
CD4T memory cells	0.084	0.081	0.079	0.535	0.599	0.639	0.531	0.410	0.686
B memory cells	0.019	0.017	0.019	1.287	0.214	-0.457	0.653	-1.380	0.184
B naive cells	0.040	0.035	0.046	1.611	0.125	-2.018	0.059	-3.907	**0.001**
T regulatory cells	0.005	0.007	0.008	-0.978	0.341	-1.946	0.067	-0.842	0.411
CD8T memory cells	0.051	0.052	0.049	-0.290	0.775	0.359	0.724	0.650	0.524
CD8T naive cells	0.025	0.028	0.026	-1.354	0.193	-0.456	0.654	0.607	0.552
Eosinophiles	0.009	0.009	0.005	0.306	0.763	1.400	0.178	1.036	0.314
Natural Killer	0.044	0.047	0.048	-0.696	0.495	-1.046	0.309	-0.339	0.739
Neutrophiles	0.564	0.575	0.556	-0.612	0.548	0.309	0.761	0.966	0.347
Monocytes	0.062	0.053	0.082	2.282	**0.035**	-3.415	**0.003**	-5.527	**$3.0 \cdot 10^{-5}$**

The first three columns show the mean values for each immune cell proportion at each time point. The next columns have information about the t-test between baseline and 3-month test, between baseline and 6-month test, and between 3-month and 6-month tests, respectively. In bold, the significant associations are highlighted. The means of each cell type are reported as relative cell percentages in decimal format.

Table 5. Statistical analysis for comparing baseline and 6-month immune cell proportions in the Dasatinib, Quercetin, and Fisetin study.

	Mean		Baseline vs 6-month	
	Baseline	6-month	T-score	P-value
CD4T naive cells	0.065	0.063	0.200	0.844
Basophiles	0.014	0.013	0.507	0.618
CD4T memory cells	0.081	0.089	-0.926	0.367
B memory cells	0.017	0.015	1.122	0.277
B naive cells	0.040	0.024	4.470	**$3.0 \cdot 10^{-4}$**
T regulatory cells	0.006	0.004	2.069	0.053
CD8T memory cells	0.063	0.058	0.950	0.354
CD8T naive cells	0.020	0.017	1.202	0.245
Eosinophiles	0.011	0.011	-0.009	0.993
Natural Killer	0.055	0.048	1.620	0.123
Neutrophiles	0.569	0.597	-1.336	0.198
Monocytes	0.060	0.062	-0.421	0.679

The first two columns show the mean values for each immune cell proportion at each time point. The next columns have information about the t-test between baseline and 6-month test. In bold, the significant associations are highlighted. The means of each cell type are reported as relative cell percentages in decimal format.

In conjunction with our findings, prior studies underscore that first-generation clocks, exemplified by the Skin and blood clock, exhibit an increase with cell passage and time in cell culture, regardless of human telomerase reverse transcriptase (hTERT) expression [50]. This observation raises questions about the efficacy of epigenetic age clocks in precisely measuring the processes and biological impact of senescence.

While the link between cellular senescence and aging is indisputable [51], the differential analysis of these clocks limits our interpretation of their clinical significance. However, the advantages of senolytic treatments have shown greater nuances, as detrimental and sex-based effects have been seen in mice [52]. Indeed, previous literature has shown varied benefits among mice models and human trials with the application of senolytics [53, 54]. The non-significant change in second and third-generation clocks such as GrimAge and DunedinPACE further emphasizes the potential of these clocks, trained to phenotypes of aging, are more prone to capture the underlying biology of aging since these are trained to biomarkers, to capture the underlying biology of aging. It is plausible that the significant biological age increases seen in first-generation clocks and DNAmPhenoAge might be attributed to age-correlated CpG locations rather than underlying biological impacts, as the more predictive and biologically associated second and third-generation clocks do not exhibit a similar increase. This pattern underscores the need for cautious interpretation, as different generations of clocks may reflect diverse interventional changes, as observed in previous studies like the CALERIE study, where caloric restriction impacted aging changes significantly only in DunedinPACE [55].

The inclusion of Fisetin in the second study revealed differences in the effects of senolytic drugs upon epigenetic aging compared to the first study. While DQ increased both first-generation clocks and PhenoAge, only PC Horvath pan tissue showed a significant increase in the DQF group. This discrepancy suggests
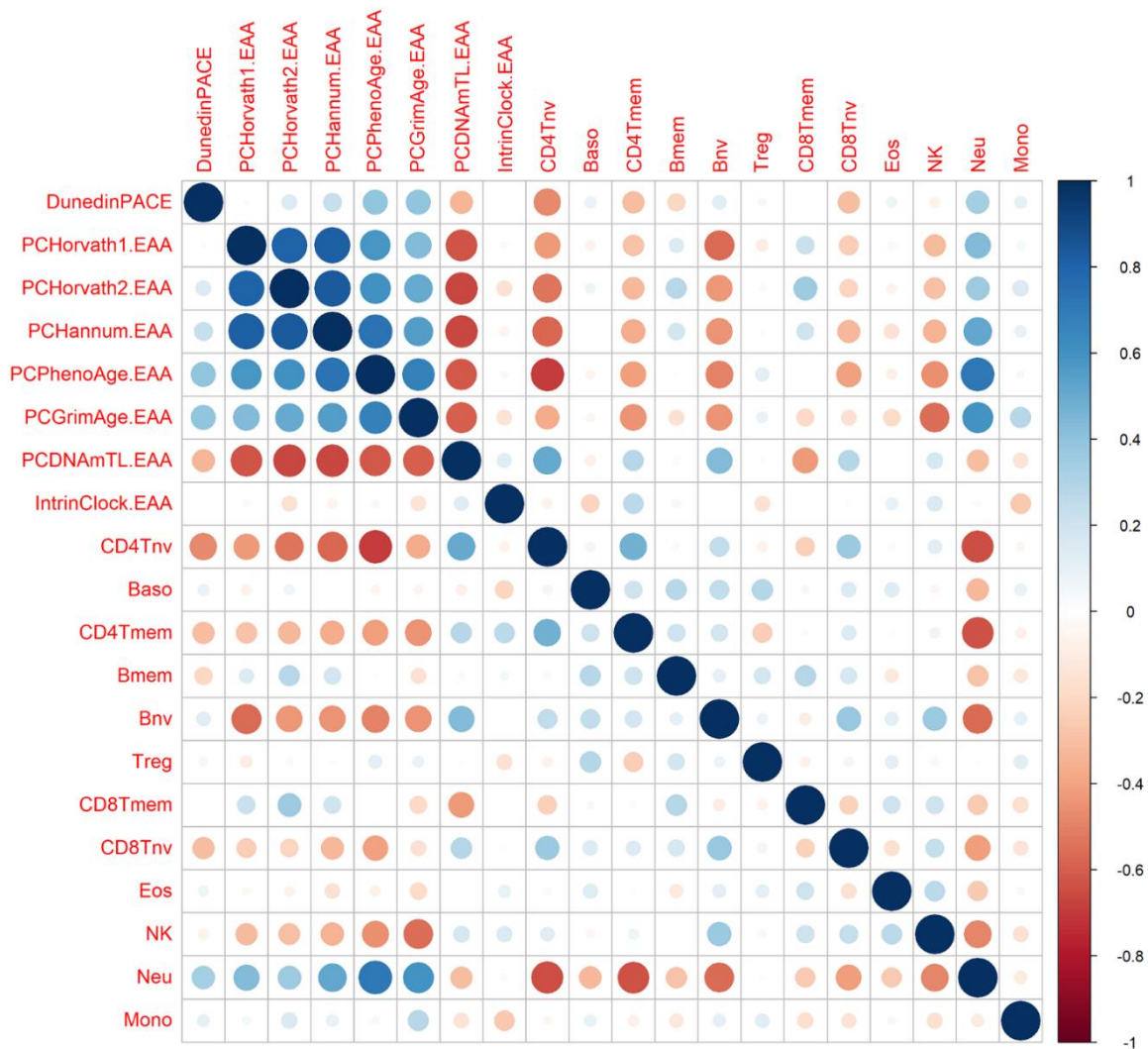
Figure 5. Correlation between epigenetic clocks and immune cell types. The size of the dots is proportional to the correlation value, being blue a positive correlation and red a negative correlation.

Table 6. Inflammation and inflammatory proteomic EpiScore analysis between baseline, 3-month test, and 6-month test in the Dasatinib and Quercetin (DQ) trial.

| | Mean | | | Baseline vs 3-month | | Baseline vs 6-month | | 3-month vs 6-month | |
	Base	3m	6m	T-score	P-value	T-score	P-value	T-score	P-value
CCL11	-0.007	-0.007	-0.004	0.071	0.944	-2.94	**0.009**	-3.97	**0.001**
CCL17	-0.434	-0.428	-0.435	-3.306	**0.004**	1.062	0.302	3.614	**0.002**
CCL18	-0.15	-0.15	-0.148	0.002	0.998	-1.443	0.166	-1.722	0.102
CCL21	-0.127	-0.128	-0.127	1.449	0.165	0.06	0.953	-1.473	0.158
CCL22	-0.066	-0.065	-0.064	-0.428	0.674	-3.241	**0.005**	-3.269	**0.004**
Complement C4	0.032	0.031	0.033	2.923	**0.009**	-1.723	0.102	-4.513	**$2.7 \cdot 10^{-4}$**
Complement C5a	0.155	0.148	0.158	3.721	**0.002**	-2.268	**0.036**	-6.877	**$2.0 \cdot 10^{-5}$**
Complement C9	-0.013	-0.012	-0.011	-0.545	0.592	-0.751	0.462	-0.229	0.822
CRP	-0.114	-0.107	-0.115	-4.888	**$1.2 \cdot 10^{-4}$**	0.979	0.34	4.679	**$1.9 \cdot 10^{-4}$**
CXCL10 soma	-0.345	-0.338	-0.343	-2.939	**0.009**	-0.966	0.347	1.911	0.072
CXCL11 soma	-0.053	-0.05	-0.054	-3.291	**0.004**	1.282	0.216	5.23	**$5.7 \cdot 10^{-5}$**
CXCL9	-0.034	-0.031	-0.037	-3.347	**0.004**	2.728	**0.014**	5.132	**$7.0 \cdot 10^{-5}$**
Interleukin 19	-0.002	-0.005	-0.005	1.064	0.302	1.241	0.231	0.188	0.853
TGF alpha	0.021	0.026	0.018	-2.842	**0.011**	1.29	0.213	3.989	**0.001**
TNFRSF1B	-0.106	-0.104	-0.105	-1.898	0.074	-1.028	0.317	0.525	0.606
Relative IL6 Level	-0.079	-0.086	-0.041	0.501	0.622	-2.495	**0.023**	-3.292	**0.004**

The first three columns show the mean values for each protein methylation risk score (MRS) at each time point. The next columns have information about the t-test between baseline and 3-month test, between baseline and 6-month test, and between 3-month and 6-month tests, respectively.

that Fisetin's additional benefits beyond senolytic activity, such as improved cognitive function and neuroprotection [56, 57], might have modulated DQ's effect on epigenetic clocks. To definitively isolate the specific effects of each treatment, future studies should investigate Fisetin without DQ.

A main confounding variable which limits our ability to establish biological aging significance is the significant changes in CD4T and CD8T Naive cells, B Naive cells, and monocytes. Immune cell changes with aging have been a large confounding error in previous DNAm clocks. For instance, previous studies have shown that human naive CD8+ T cells can exhibit an epigenetic age 15–20 years younger than effector memory CD8+ T cells from the same individual. This means that previous epigenetic clocks measure two independent variables, aging and immune cell composition tomu [58]. To analyze if immune changes were responsible for the first-generation epigenetic clock acceleration, we calculated immune EAA and adjusted by all the immune cells that were significantly associated to the clocks (CD4T naive and memory cells, B naive and memory cells, CD8T naive and memory cells, natural killers, and neutrophils). We found that the significance and direction of the associations were not modified after adjusting by immune cells, indicating that the increase of epigenetic age after DQ treatment was not due to the modulation of immune cell subsets but representing an

increase due to the CpG inclusion and weights of the clocks themselves. In addition, we included the IntrinClock to assess the epigenetic age which is independent of immune cell subset changes. This clock showed no significant change in any of the treatment arms. One source for this result could be due to the unique construction for the IntrinClock, which was generated via the deliberate removal of CpGs that were characteristic of naïve cells. It is possible that senolytic treatment is affecting a subset of CpGs that were removed in the construction of the IntrinClock that are more correlated to general properties of naïve cells (quiescence, etc.) rather than those that represent immune cell type composition specifically.

The major hypothesized mechanism for the negative impacts of senescence is through the increased senescence-associated secretory phenotypes (SASP) which lead to high inflammatory cytokine signaling from senescent cells in a paracrine fashion. Although SASP proteins were not measured directly in this study, we used DNA methylation risk scores for protein surrogates to analyze changes in common SASP proteins. In some cases, these methylation risk scores have been shown to have better resolution and connection to outcomes than traditional measures. For instance, the Episcore for C-Reactive protein has shown age-related associations in cohorts which were not seen with log(CRP) clinical measures and association to

cognitive function and brain MRIs [59]. Looking at these methylation risk scores in our longitudinal data, we see some interesting trends of increased inflammatory mediators at 3 months which decrease from the 3-6 month timepoints. These inflammatory-associated proteins include CRP, CXCL9, CXCL11, CCL17, and TGF-alpha. We see opposite trends with other inflammation-associated markers such as Complement C4 and Complement C5a. The accuracy of the EpiScore protein predictions to measured proteins is still low. Thus, the changes we see here are limited by the accuracy of the prediction. CRP, which is the most validated of the proteomic EpiSign scores, shows decreases at 3 months and increases at 6 months which might suggest duration of senolytic therapy might impact the phenotypic outcomes. Furthermore, the treatment impacts on the SASP might also indicate a plausible explanation for the differences in age accelerations between the first-generation IntrinClock and other first-generation clocks. SASP-related CpG sites would be differentially methylated in naïve T cells and thus removed from the construction of the IntrinClock but not Horvath, Hannum, or PhenoAge clocks.

Finally, telomere and mitotic clock outputs showed a significant reduction in telomere lengths and increases in mitotic clock values. While this suggests a contradictory notion that cell cycle replication increased and relative leukocyte telomere levels decreased, histology combined with senescence marker staining (e.g., β-Galactosidase) will be needed to support these conclusions. Therefore, further investigations with paired histology are needed to better assess the impact of senolytics on telomere lengths and cell cycle.

In summary, our findings underscore the imperative for additional markers to gauge the physiological impact of senolytic treatments, emphasizing the critical need for developing new biomarkers to quantify senescence and its effects on aging. This is exemplified by the incongruence between first-generation, second-generation, and third-generation clock outputs that are shown here. Beyond biological age, there is also a need to improve upon certain methylation surrogate predictors, as some SASP proteins exhibit changes that are contrary to current dogma. Strengths of the present study include its prospective longitudinal design, the duration of longitudinal measures, the standardized and batch normalized epigenetic data, and comprehensive inclusion of novel and complementary epigenetic age measures that were repeatedly collected. Notwithstanding, limitations such as a modest sample size, absence of a control group, and exclusive measurement in blood samples underscore the necessity for cautious interpretation and advocate for future studies with larger

cohorts, diverse biomarkers, and tissue-specific analyses to augment comprehension of senolytic therapy effects. We hope this data can be reanalyzed as new senolytic DNA methylation analysis tools become available.

MATERIALS AND METHODS

Study participants and senolytic administration

For the evaluation of DQ treatment upon epigenetic age, 19 study participants were accrued from November 2020 to December 2020 at the Institute for Hormonal Balance, Orlando. The sample size was determined for the pilot study based on individuals who were willing to participate in the research. Table 1 shows the demographic and clinical characteristics of these participants. Adults aged 40 and older able to comply with treatment plan and laboratory tests were included. Individuals with neoplastic cancer within 5 years prior to screening, immune disease, viral illness, cardio-vascular or cerebrovascular disease, ischemic attack in the last 6 months, hepatitis or HIV, Body mass index higher than 40kg/m2, active infection, or previously used DQ were excluded. Informed consent was obtained from study participants. The FDA registered IRB (Institute for Regenerative and Cellular Medicine) approved this study, which is registered at ClinicalTrials.gov (NCT04946383) and which is an ongoing clinical trial to determine the effectiveness of Quercetin and Dasatinib supplements on the patient's epigenetic aging rate. The treatment comprised 500mg Quercetin and 50mg Dasatinib oral capsules on Monday, Tuesday, and Wednesday (3 days in a row) per month for the duration of 6 months. Blood was collected at baseline, at the middle of the study (3 months), and at the end of the study (6 months). It is worth mentioning that three subjects stopped the treatment after 3 months due to nausea, prostate cancer diagnosis, and concern about the drug, respectively.

For the evaluation of DQF treatment, all the participants from the first study were invited to join and new participants were recruited from June 2022 to July 2022 at the Institute for Hormonal Balance, Orlando. From the previous study, 10 participants joined this study, and 9 participants were newly recruited. The same inclusion and exclusion criteria were followed as in the DQ study. In this case, the treatment consisted of the same dosage and timeline as in the DQ treatment but included 500 mg of Fisetin oral capsules on Monday, Tuesday, and Wednesday (3 days in a row) per month for the duration of 6 months. Moreover, 8 participants got a strawberry based Fisetin and 11 got a non-strawberry based Fisetin. Blood was collected at baseline and at the end of the study (6 months).

DNA methylation assessment

Peripheral whole blood samples were obtained using the lancet and capillary method and immediately mixed with lysis buffer to preserve the cells. DNA extraction was performed, and 500 ng of DNA was subjected to bisulfite conversion using the EZ DNA Methylation kit from Zymo Research, following the manufacturer's protocol. The bisulfite-converted DNA samples were then randomly allocated to designated wells on the Infinium HumanMethylationEPIC BeadChip. The samples were amplified, hybridized onto the array, and subsequently stained. After washing steps, the array was imaged using the Illumina iScan SQ instrument to capture raw image intensities, enabling further analysis.

Minfi R package was used for the pre-processing of DNAm data. We pre-processed all the samples from the different studies together to remove batch effects. In the sample quality control, we removed those samples with aberrant methylation levels and with background signal levels (mean p-value higher than 0.05). We also discarded those probes with background signal following the same threshold. We further normalized the methylation values using the Genome-wide Median Normalization (GMQN) and the Beta Mixture Quantile (BMIQ) methods. Finally, we imputed the missing values using the k-nearest neighbors (knn) algorithm. Finally, we used a 12-cell immune deconvolution method developed by Zhend et al. to estimate cell type proportions. We chose this method because in previous analysis we saw this has R^2 of 0.96 and above to immune cell subsets measured by RNA-seq and flow cytometry [60].

Statistical analyses and reproducibility

DNA methylation clocks and related measures
We used DNAm data to calculate a series of measures broadly known as epigenetic clocks. We computed four clocks designed to predict the chronological age of the donor, Horvath Pan Tissue, Horvath Skin and Blood, and Hannum; two clocks designed to predict mortality, the DNAmPhenoAge and GrimAge clocks; a clock to measure telomere length, DNAmTL [36]; two clock designed to measure mitotic age, total stem cell divisions (tnsc) and intrinsic tissue stem cell division (irS) [61]; a DNAm measure of the rate of deterioration in physiological integrity, the DundedinPACE; and a clock to measure chronological age but not dependent on immune cells, the IntrinClock.

To calculate the principal component-based epigenetic clock for the Horvath multi-tissue clock, Hannum clock, DNAmPhenoAge clock, GrimAge clock, and telomere length we used the custom R script available via GitHub

(https://github.com/MorganLevineLab/PC-Clocks). Non-principal component-based (non-PC) Horvath, Hannum, and DNAmPhenoAge epigenetic metrics were calculated using the methyAge function in the ENMix R package. The pace of aging clock, DunedinPACE, was calculated using the PACEProjector function from the DunedinPACE package available via GitHub (https://github.com/danbelsky/DunedinPACE). The mitotic clocks were calculated using the epiTOC2 function from the meffonym package. Finally, the IntrinClock was calculated as described elsewhere [58].

To calculate the EAA of multiple clocks, we fit a regression model between the chronological age of the individuals and the different epigenetic age measures. We also included the batch PCs as a fixed effect as a way to control for potential batch effects. This methodology of incorporating PCs in EAA calculations was previously described in Joyce et al. Paired t-tests were performed using EAA values between timepoints at a significance level of $p < 0.05$.

Differentially methylated loci analysis
The epigenome-wide association study (EWAS) was performed using the limma Bioconductor package. We performed a differential mean analysis on different timepoints to see whether the treatment was associated with changes at specific loci. Based on the available covariates, we adjusted all the regression models by sex, age, batch effect, and three principal components. We also set as random effect the participant ID. For each timepoint comparison, we fitted models

$$E_j = \alpha_j + \beta_j S + \Sigma \gamma_r C_r + \varepsilon_j \tag{1}$$

where E_j denotes the methylation level vector across individuals at probe j (j = 1, . . . 866836), S is the time point with its associated effect, β_j, C_r is the r adjusting covariate and its effect γ_r, and ε_j is the noise that follows the distribution of methylation levels with mean 0. Adjusted P-values were calculated using FDR correction for considering multiple comparisons. The inflation or deflation of P-values across the methylome was assessed with Q-Q plots and lambda values. We selected as significant probes those with FDR lower than 0.05 after correcting for multiple comparisons.

We next used GREAT to understand the functional relevance of the differentially methylated loci (DML) with a nominal p-value lower than $1 \cdot 10^{-4}$. The GREAT software will compare genomic features against the genes of interest in order to run Gene Ontology (GO) analysis. This software looks at the number of DMLs which overlap to the promoter and enhancer regions to run a binomial enrichment analysis of identifying overrepresented/enriched GO terms.

AUTHOR CONTRIBUTIONS

EL performed patient recruitment, clinical management, and sample procurement. NC and VD performed methylation preprocessing, data analysis, and statistical analysis. EV and AT analyzed IntrinClock data. LN and MC provided immune cell subset analysis. TM conducted methylation laboratory analysis. HW, AL, LT, LL, and RS helped with study design, manuscript drafting, and submission.

ACKNOWLEDGMENTS

CONFLICTS OF INTEREST

NC, VBD, RS, HW, AL, LT, and TLM are employees of TruDiagnostic.

ETHICAL STATEMENT AND CONSENT

The study involving human participants was reviewed and approved by the Institute for Regenerative and Cellular Medicine and registered at ClinicalTrials.gov (NCT04946383). The participants provided informed consent to participate in this study.

FUNDING

REFERENCES

1. Hayflick L. The limited *in vitro* lifetime of human diploid cell strains. Exp Cell Res. 1965; 37:614–36.
   https://doi.org/10.1016/0014-4827(65)90211-9
   PMID:14315085

2. Tchkonia T, Zhu Y, van Deursen J, Campisi J, Kirkland JL. Cellular senescence and the senescent secretory phenotype: therapeutic opportunities. J Clin Invest. 2013; 123:966–72.
   https://doi.org/10.1172/JCI64098 PMID:23454759

3. Campisi J, d'Adda di Fagagna F. Cellular senescence: when bad things happen to good cells. Nat Rev Mol Cell Biol. 2007; 8:729–40.
   https://doi.org/10.1038/nrm2233 PMID:17667954

4. Kang C. Senolytics and Senostatics: A Two-Pronged Approach to Target Cellular Senescence for Delaying Aging and Age-Related Diseases. Mol Cells. 2019; 42:821–27.
   https://doi.org/10.14348/molcells.2019.0298
   PMID:31838837

5. Gorgoulis V, Adams PD, Alimonti A, Bennett DC, Bischof O, Bishop C, Campisi J, Collado M, Evangelou K, Ferbeyre G, Gil J, Hara E, Krizhanovsky V, et al. Cellular Senescence: Defining a Path Forward. Cell. 2019; 179:813–27.
   https://doi.org/10.1016/j.cell.2019.10.005
   PMID:31675495

6. He S, Sharpless NE. Senescence in Health and Disease. Cell. 2017; 169:1000–11.
   https://doi.org/10.1016/j.cell.2017.05.015
   PMID:28575665

7. Xu M, Pirtskhalava T, Farr JN, Weigand BM, Palmer AK, Weivoda MM, Inman CL, Ogrodnik MB, Hachfeld CM, Fraser DG, Onken JL, Johnson KO, Verzosa GC, et al. Senolytics improve physical function and increase lifespan in old age. Nat Med. 2018; 24:1246–56.
   https://doi.org/10.1038/s41591-018-0092-9
   PMID:29988130

8. Xu M, Bradley EW, Weivoda MM, Hwang SM, Pirtskhalava T, Decklever T, Curran GL, Ogrodnik M, Jurk D, Johnson KO, Lowe V, Tchkonia T, Westendorf JJ, Kirkland JL. Transplanted Senescent Cells Induce an Osteoarthritis-Like Condition in Mice. J Gerontol A Biol Sci Med Sci. 2017; 72:780–5.
   https://doi.org/10.1093/gerona/glw154
   PMID:27516624

9. López-Otín C, Blasco MA, Partridge L, Serrano M, Kroemer G. Hallmarks of aging: An expanding universe. Cell. 2023; 186:243–78.
   https://doi.org/10.1016/j.cell.2022.11.001
   PMID:36599349

10. Guo J, Huang X, Dou L, Yan M, Shen T, Tang W, Li J. Aging and aging-related diseases: from molecular mechanisms to interventions and treatments. Signal Transduct Target Ther. 2022; 7:391.
    https://doi.org/10.1038/s41392-022-01251-0
    PMID:36522308

11. Kennedy BK, Berger SL, Brunet A, Campisi J, Cuervo AM, Epel ES, Franceschi C, Lithgow GJ, Morimoto RI, Pessin JE, Rando TA, Richardson A, Schadt EE, et al. Geroscience: linking aging to chronic disease. Cell. 2014; 159:709–13.
    https://doi.org/10.1016/j.cell.2014.10.039
    PMID:25417146

12. Kirkland JL, Tchkonia T. Senolytic drugs: from discovery to translation. J Intern Med. 2020; 288:518–36.
    https://doi.org/10.1111/joim.13141
    PMID:32686219

13. Gnoni A, Marech I, Silvestris N, Vacca A, Lorusso V.

Dasatinib: an anti-tumour agent via Src inhibition. Curr Drug Targets. 2011; 12:563–78.
https://doi.org/10.2174/138945011794751591
PMID:21226671

14. Ichwan M, Walker TL, Nicola Z, Ludwig-Müller J, Böttcher C, Overall RW, Adusumilli VS, Bulut M, Sykes AM, Hübner N, Ramirez-Rodriguez G, Ortiz-López L, Lugo-Hernández EA, Kempermann G. Apple Peel and Flesh Contain Pro-neurogenic Compounds. Stem Cell Reports. 2021; 16:548–65.
https://doi.org/10.1016/j.stemcr.2021.01.005
PMID:33577796

15. Khan N, Syed DN, Ahmad N, Mukhtar H. Fisetin: a dietary antioxidant for health promotion. Antioxid Redox Signal. 2013; 19:151–62.
https://doi.org/10.1089/ars.2012.4901
PMID:23121441

16. Wissler Gerdes EO, Zhu Y, Tchkonia T, Kirkland JL. Discovery, development, and future application of senolytics: theories and predictions. FEBS J. 2020; 287:2418–27.
https://doi.org/10.1111/febs.15264 PMID:32112672

17. Hickson LJ, Langhi Prata LGP, Bobart SA, Evans TK, Giorgadze N, Hashmi SK, Herrmann SM, Jensen MD, Jia Q, Jordan KL, Kellogg TA, Khosla S, Koerber DM, et al. Senolytics decrease senescent cells in humans: Preliminary report from a clinical trial of Dasatinib plus Quercetin in individuals with diabetic kidney disease. EBioMedicine. 2019; 47:446–56.
https://doi.org/10.1016/j.ebiom.2019.08.069
PMID:31542391

18. Islam MT, Tuday E, Allen S, Kim J, Trott DW, Holland WL, Donato AJ, Lesniewski LA. Senolytic drugs, dasatinib and quercetin, attenuate adipose tissue inflammation, and ameliorate metabolic function in old age. Aging Cell. 2023; 22:e13767.
https://doi.org/10.1111/acel.13767 PMID:36637079

19. Ijima S, Saito Y, Nagaoka K, Yamamoto S, Sato T, Miura N, Iwamoto T, Miyajima M, Chikenji TS. Fisetin reduces the senescent tubular epithelial cell burden and also inhibits proliferative fibroblasts in murine lupus nephritis. Front Immunol. 2022; 13:960601.
https://doi.org/10.3389/fimmu.2022.960601
PMID:36466895

20. Hambright WS, Mu X, Gao X, Guo P, Kawakami Y, Mitchell J, Mullen M, Nelson AL, Bahney C, Nishimura H, Hellwinkel J, Eck A, Huard J. The Senolytic Drug Fisetin Attenuates Bone Degeneration in the Zmpste24$^{-/-}$ Progeria Mouse Model. J Osteoporos. 2023; 2023:5572754.
https://doi.org/10.1155/2023/5572754
PMID:36875869

21. Schafer MJ, White TA, Iijima K, Haak AJ, Ligresti G,

Atkinson EJ, Oberg AL, Birch J, Salmonowicz H, Zhu Y, Mazula DL, Brooks RW, Fuhrmann-Stroissnigg H, et al. Cellular senescence mediates fibrotic pulmonary disease. Nat Commun. 2017; 8:14532.
https://doi.org/10.1038/ncomms14532
PMID:28230051

22. Novais EJ, Tran VA, Johnston SN, Darris KR, Roupas AJ, Sessions GA, Shapiro IM, Diekman BO, Risbud MV. Long-term treatment with senolytic drugs Dasatinib and Quercetin ameliorates age-dependent intervertebral disc degeneration in mice. Nat Commun. 2021; 12:5213.
https://doi.org/10.1038/s41467-021-25453-2
PMID:34480023

23. Ruggiero AD, Vemuri R, Blawas M, Long M, DeStephanis D, Williams AG, Chen H, Justice JN, Macauley SL, Day SM, Kavanagh K. Long-term dasatinib plus quercetin effects on aging outcomes and inflammation in nonhuman primates: implications for senolytic clinical trial design. Geroscience. 2023; 45:2785–803.
https://doi.org/10.1007/s11357-023-00830-5
PMID:37261678

24. Gasek NS, Kuchel GA, Kirkland JL, Xu M. Strategies for Targeting Senescent Cells in Human Disease. Nat Aging. 2021; 1:870–9.
https://doi.org/10.1038/s43587-021-00121-8
PMID:34841261

25. Afroze N, Pramodh S, Shafarin J, Bajbouj K, Hamad M, Sundaram MK, Haque S, Hussain A. Fisetin Deters Cell Proliferation, Induces Apoptosis, Alleviates Oxidative Stress and Inflammation in Human Cancer Cells, HeLa. Int J Mol Sci. 2022; 23:1707.
https://doi.org/10.3390/ijms23031707
PMID:35163629

26. Yousefzadeh MJ, Zhu Y, McGowan SJ, Angelini L, Fuhrmann-Stroissnigg H, Xu M, Ling YY, Melos KI, Pirtskhalava T, Inman CL, McGuckian C, Wade EA, Kato JI, et al. Fisetin is a senotherapeutic that extends health and lifespan. EBioMedicine. 2018; 36:18–28.
https://doi.org/10.1016/j.ebiom.2018.09.015
PMID:30279143

27. Bell CG, Lowe R, Adams PD, Baccarelli AA, Beck S, Bell JT, Christensen BC, Gladyshev VN, Heijmans BT, Horvath S, Ideker T, Issa JJ, Kelsey KT, et al. DNA methylation aging clocks: challenges and recommendations. Genome Biol. 2019; 20:249.
https://doi.org/10.1186/s13059-019-1824-y
PMID:31767039

28. Bergsma T, Rogaeva E. DNA Methylation Clocks and Their Predictive Capacity for Aging Phenotypes and Healthspan. Neurosci Insights. 2020;

15:2633105520942221.
https://doi.org/10.1177/2633105520942221
PMID:32743556

29. Horvath S. DNA methylation age of human tissues and cell types. Genome Biol. 2013; 14:R115.
https://doi.org/10.1186/gb-2013-14-10-r115
PMID:24138928

30. Hannum G, Guinney J, Zhao L, Zhang L, Hughes G, Sadda S, Klotzle B, Bibikova M, Fan JB, Gao Y, Deconde R, Chen M, Rajapakse I, et al. Genome-wide methylation profiles reveal quantitative views of human aging rates. Mol Cell. 2013; 49:359–67.
https://doi.org/10.1016/j.molcel.2012.10.016
PMID:23177740

31. Levine ME, Lu AT, Quach A, Chen BH, Assimes TL, Bandinelli S, Hou L, Baccarelli AA, Stewart JD, Li Y, Whitsel EA, Wilson JG, Reiner AP, et al. An epigenetic biomarker of aging for lifespan and healthspan. Aging (Albany NY). 2018; 10:573–91.
https://doi.org/10.18632/aging.101414
PMID:29676998

32. Lu AT, Quach A, Wilson JG, Reiner AP, Aviv A, Raj K, Hou L, Baccarelli AA, Li Y, Stewart JD, Whitsel EA, Assimes TL, Ferrucci L, Horvath S. DNA methylation GrimAge strongly predicts lifespan and healthspan. Aging (Albany NY). 2019; 11:303–27.
https://doi.org/10.18632/aging.101684
PMID:30669119

33. Belsky DW, Caspi A, Corcoran DL, Sugden K, Poulton R, Arseneault L, Baccarelli A, Chamarti K, Gao X, Hannon E, Harrington HL, Houts R, Kothari M, et al. DunedinPACE, a DNA methylation biomarker of the pace of aging. Elife. 2022; 11:e73420.
https://doi.org/10.7554/eLife.73420
PMID:35029144

34. Jonkman TH, Dekkers KF, Slieker RC, Grant CD, Ikram MA, van Greevenbroek MMJ, Franke L, Veldink JH, Boomsma DI, Slagboom PE, Consortium BI, Heijmans BT. Functional genomics analysis identifies T and NK cell activation as a driver of epigenetic clock progression. Genome Biol. 2022; 23:24.
https://doi.org/10.1186/s13059-021-02585-8
PMID:35031073

35. Victorelli S, Passos JF. Telomeres and Cell Senescence - Size Matters Not. EBioMedicine. 2017; 21:14–20.
https://doi.org/10.1016/j.ebiom.2017.03.027
PMID:28347656

36. Lu AT, Seeboth A, Tsai PC, Sun D, Quach A, Reiner AP, Kooperberg C, Ferrucci L, Hou L, Baccarelli AA, Li Y, Harris SE, Corley J, et al. DNA methylation-based estimator of telomere length. Aging (Albany NY). 2019; 11:5895–923.

37. Zerlanko BJ, Bartholin L, Melhuish TA, Wotton D. Premature senescence and increased TGFβ signaling in the absence of Tgif1. PLoS One. 2012; 7:e35460.
https://doi.org/10.1371/journal.pone.0035460
PMID:22514746

38. Liesenfeld M, Mosig S, Funke H, Jansen L, Runnebaum IB, Dürst M, Backsch C. SORBS2 and TLR3 induce premature senescence in primary human fibroblasts and keratinocytes. BMC Cancer. 2013; 13:507.
https://doi.org/10.1186/1471-2407-13-507
PMID:24165198

39. Villot R, Poirier A, Bakan I, Boulay K, Fernández E, Devillers R, Gama-Braga L, Tribouillard L, Gagné A, Duchesne É, Caron D, Bérubé JS, Bérubé JC, et al. ZNF768 links oncogenic RAS to cellular senescence. Nat Commun. 2021; 12:4841.
https://doi.org/10.1038/s41467-021-24932-w
PMID:34404770

40. Wiley CD, Campisi J. From Ancient Pathways to Aging Cells-Connecting Metabolism and Cellular Senescence. Cell Metab. 2016; 23:1013–21.
https://doi.org/10.1016/j.cmet.2016.05.010
PMID:27304503

41. Shin EY, Soung NK, Schwartz MA, Kim EG. Altered endocytosis in cellular senescence. Ageing Res Rev. 2021; 68:101332.
https://doi.org/10.1016/j.arr.2021.101332
PMID:33753287

42. Moujaber O, Fishbein F, Omran N, Liang Y, Colmegna I, Presley JF, Stochaj U. Cellular senescence is associated with reorganization of the microtubule cytoskeleton. Cell Mol Life Sci. 2019; 76:1169–83.
https://doi.org/10.1007/s00018-018-2999-1
PMID:30599068

43. Muñoz-Espín D, Cañamero M, Maraver A, Gómez-López G, Contreras J, Murillo-Cuesta S, Rodríguez-Baeza A, Varela-Nieto I, Ruberte J, Collado M, Serrano M. Programmed cell senescence during mammalian embryonic development. Cell. 2013; 155:1104–18.
https://doi.org/10.1016/j.cell.2013.10.019
PMID:24238962

44. Abbadie C, Pluquet O, Pourtier A. Epithelial cell senescence: an adaptive response to pre-carcinogenic stresses? Cell Mol Life Sci. 2017; 74:4471–509.
https://doi.org/10.1007/s00018-017-2587-9
PMID:28707011

45. Valenzuela CA, Quintanilla R, Moore-Carrasco R, Brown NE. The Potential Role of Senescence As a Modulator of Platelets and Tumorigenesis. Front Oncol. 2017; 7:188.
https://doi.org/10.3389/fonc.2017.00188
PMID:28894697

46. Krouwer VJD, Hekking LHP, Langelaar-Makkinje M, Regan-Klapisz E, Post JA. Endothelial cell senescence is associated with disrupted cell-cell junctions and increased monolayer permeability. Vasc Cell. 2012; 4:12.
https://doi.org/10.1186/2045-824X-4-12
PMID:22929066

47. Chen MS, Lee RT, Garbern JC. Senescence mechanisms and targets in the heart. Cardiovasc Res. 2022; 118:1173–87.
https://doi.org/10.1093/cvr/cvab161 PMID:33963378

48. Gadd DA, Hillary RF, McCartney DL, Zaghlool SB, Stevenson AJ, Cheng Y, Fawns-Ritchie C, Nangle C, Campbell A, Flaig R, Harris SE, Walker RM, Shi L, et al. Epigenetic scores for the circulating proteome as tools for disease prediction. Elife. 2022; 11:e71802.
https://doi.org/10.7554/eLife.71802
PMID:35023833

49. Levine ME, Higgins-Chen A, Thrush K, Minteer C, Niimi P. Clock Work: Deconstructing the Epigenetic Clock Signals in Aging, Disease, and Reprogramming. bioRxiv. 2022; 2022.02.13.480245.
https://doi.org/10.1101/2022.02.13.480245

50. Kabacik S, Lowe D, Fransen L, Leonard M, Ang SL, Whiteman C, Corsi S, Cohen H, Felton S, Bali R, Horvath S, Raj K. The relationship between epigenetic age and the hallmarks of aging in human cells. Nat Aging. 2022; 2:484–93.
https://doi.org/10.1038/s43587-022-00220-0
PMID:37034474

51. McHugh D, Gil J. Senescence and aging: Causes, consequences, and therapeutic avenues. J Cell Biol. 2018; 217:65–77.
https://doi.org/10.1083/jcb.201708092
PMID:29114066

52. Fang Y, Medina D, Stockwell R, McFadden S, Quinn K, Peck MR, Bartke A, Hascup KN, Hascup ER. Sexual dimorphic metabolic and cognitive responses of C57BL/6 mice to Fisetin or Dasatinib and quercetin cocktail oral treatment. Geroscience. 2023; 45:2835–50.
https://doi.org/10.1007/s11357-023-00843-0
PMID:37296266

53. Raffaele M, Vinciguerra M. The costs and benefits of senotherapeutics for human health. Lancet Healthy Longev. 2022; 3:e67–77.
https://doi.org/10.1016/S2666-7568(21)00300-7
PMID:36098323

54. Chaib S, Tchkonia T, Kirkland JL. Cellular senescence and senolytics: the path to the clinic. Nat Med. 2022; 28:1556–68.
https://doi.org/10.1038/s41591-022-01923-y
PMID:35953721

55. Waziry R, Ryan CP, Corcoran DL, Huffman KM, Kobor MS, Kothari M, Graf GH, Kraus VB, Kraus WE, Lin DT, Pieper CF, Ramaker ME, Bhapkar M, et al. Effect of long-term caloric restriction on DNA methylation measures of biological aging in healthy adults from the CALERIE trial. Nat Aging. 2023; 3:248–57.
https://doi.org/10.1038/s43587-022-00357-y
PMID:37118425

56. Hassan SS, Samanta S, Dash R, Karpiński TM, Habibi E, Sadiq A, Ahmadi A, Bunagu S. The neuroprotective effects of fisetin, a natural flavonoid in neurodegenerative diseases: Focus on the role of oxidative stress. Front Pharmacol. 2022; 13:1015835.
https://doi.org/10.3389/fphar.2022.1015835
PMID:36299900

57. Nabavi SF, Braidy N, Habtemariam S, Sureda A, Manayi A, Nabavi SM. Neuroprotective Effects of Fisetin in Alzheimer's and Parkinson's Diseases: From Chemistry to Medicine. Curr Top Med Chem. 2016; 16:1910–5.
https://doi.org/10.2174/1568026616666160204121725 PMID:26845554

58. Tomusiak A, Floro A, Tiwari R, Riley R, Matsui H, Andrews N. Development of a novel epigenetic clock resistant to changes in immune cell composition. bioRxiv. 2023; 2023.03.01.530561.
https://doi.org/10.1101/2023.03.01.530561

59. Conole ELS, Stevenson AJ, Muñoz Maniega S, Harris SE, Green C, Valdés Hernández MDC, Harris MA, Bastin ME, Wardlaw JM, Deary IJ, Miron VE, Whalley HC, Marioni RE, Cox SR. DNA Methylation and Protein Markers of Chronic Inflammation and Their Associations With Brain and Cognitive Aging. Neurology. 2021; 97:e2340–52.
https://doi.org/10.1212/WNL.0000000000012997
PMID:34789543

60. Luo Q, Dwaraka VB, Chen Q, Tong H, Zhu T, Seale K, Raffaele JM, Zheng SC, Mendez TL, Chen Y, Carreras N, Begum S, Mendez K, et al. A meta-analysis of immune-cell fractions at high resolution reveals novel associations with common phenotypes and health outcomes. Genome Med. 2023; 15:59.
https://doi.org/10.1186/s13073-023-01211-5
PMID:37525279

61. Christensen BC, Kelsey KT. A new timepiece: an epigenetic mitotic clock. Genome Biol. 2016; 17:216.
https://doi.org/10.1186/s13059-016-1085-y
PMID:27760549

Supplementary Figure
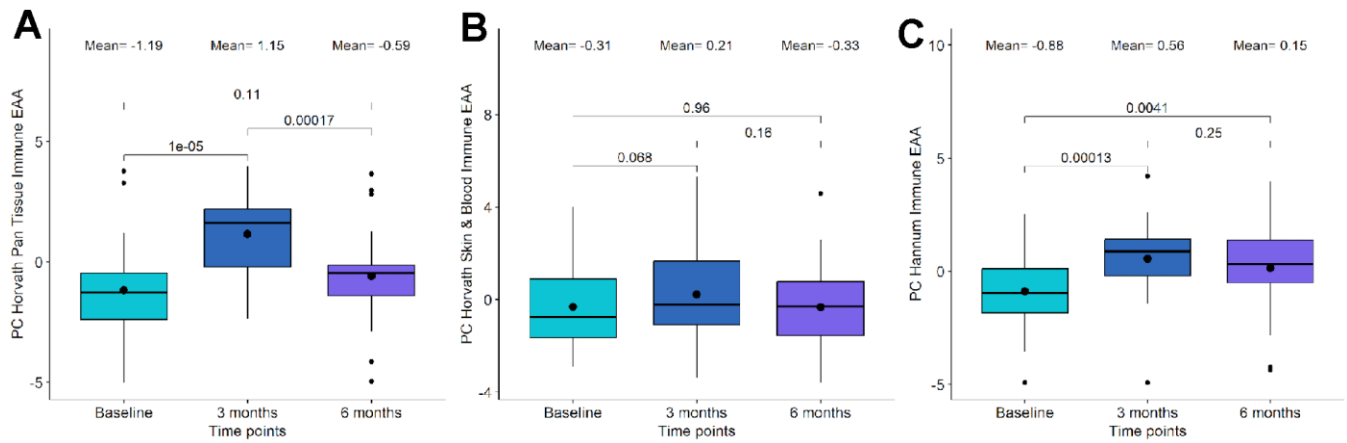
Supplementary Figure 1. Boxplot showing the evolution of epigenetic age acceleration (EAA) first-generation clocks after adjusting by immune cells in the Dasatinib and Quercetin (DQ) study. (**A**) PC Horvath pan tissue Immune EAA. (**B**) PC Horvath Skin and Blood Immune EAA. (**C**) PC Hannum Immune EAA. In the X-axis, the time points of measurements, in the Y axis, the EAA measure adjusted by immune cells. On the top, the mean values at each time point and the p-values of the paired t-tests. The box represents the interquartile range (IQR) with the median represented as a horizontal line and the mean as the dot. The vertical lines show the minimum and maximum values. When outliers are identified, those values are represented as dots.

Supplementary Tables

Please browse Full Text version to see the data of Supplementary Tables 2, 3.

Supplementary Table 1. Differentially methylated loci for Dasatinib and Quercetin (DQ) treatment and Dasatinib, Quercetin, and fisetin (DQF) treatment.

CpG site	logFC	diffMeth	P-Value	FDR	geneID
Dasatinib and Quercetin					
0-3 months					
cg05915794	0.2878	Hyper	$1.5 \cdot 10^{-12}$	$1.3 \cdot 10^{-6}$	HRNBP3
cg18889307	-0.08974	Hypo	$6.9 \cdot 10^{-9}$	0.002	TGIF1
cg02889828	-0.1833	Hypo	$8.6 \cdot 10^{-9}$	0.002	
cg27262015	-0.1243	Hypo	$2.0 \cdot 10^{-8}$	0.004	SORBS2
cg04704414	0.1107	Hyper	$1.3 \cdot 10^{-7}$	0.022	NUBP2
cg06902281	0.1175	Hyper	$1.9 \cdot 10^{-7}$	0.027	ZNF169
cg04955246	-0.155	Hypo	$2.5 \cdot 10^{-7}$	0.031	PRKCA
cg02840515	-0.1262	Hypo	$4.3 \cdot 10^{-7}$	0.039	KIAA2012
cg04132292	-0.2873	Hypo	$4.4 \cdot 10^{-7}$	0.039	
cg25024143	-0.1463	Hypo	$4.6 \cdot 10^{-7}$	0.039	SP2
cg20273352	-0.1645	Hypo	$5.6 \cdot 10^{-7}$	0.044	IGHMBP2
0-6 months					
CpG site	**logFC**	**diffMeth**	**P-Value**	**FDR**	**geneID**
cg10585661	-0.1102	Hypo	$8.0 \cdot 10^{-8}$	0.035	FAM131A
cg05779406	0.271	Hyper	$8.1 \cdot 10^{-8}$	0.035	ZFAND2A
Dasatinib, Quercetin, and Fisetin					
0-6 months					
CpG site	**logFC**	**diffMeth**	**P-Value**	**FDR**	**geneID**
cg00379708	-0.1492	Hypo	$1.4 \cdot 10^{-9}$	$6.7 \cdot 10^{-4}$	RBM20
cg13172627	0.5832	Hyper	$1.9 \cdot 10^{-9}$	$6.7 \cdot 10^{-4}$	VENTXP1
cg26676360	0.1803	Hyper	$2.3 \cdot 10^{-9}$	$6.7 \cdot 10^{-4}$	LRP1
cg02632099	0.3497	Hyper	$3.5 \cdot 10^{-9}$	$7.5 \cdot 10^{-4}$	
cg18054725	-0.1509	Hypo	$9.2 \cdot 10^{-9}$	0.002	ICAM3
cg01613010	0.2131	Hyper	$2.5 \cdot 10^{-8}$	0.002	
cg16640929	-0.6613	Hypo	$2.6 \cdot 10^{-8}$	0.002	ZBTB12
cg00877151	0.4233	Hyper	$2.8 \cdot 10^{-8}$	0.002	IPO11-LRRC70;IPO11
cg06310713	0.3591	Hyper	$3.1 \cdot 10^{-8}$	0.002	PALLD
cg08187458	0.1809	Hyper	$3.3 \cdot 10^{-8}$	0.002	
cg00288652	-0.1792	Hypo	$3.5 \cdot 10^{-8}$	0.002	
cg04706867	-0.1987	Hypo	$3.6 \cdot 10^{-8}$	0.002	CNTNAP2
cg09093137	-0.5388	Hypo	$3.7 \cdot 10^{-8}$	0.002	SRPK2
cg03012879	-0.4304	Hypo	$3.7 \cdot 10^{-8}$	0.002	HMGCR
cg12993163	-0.1746	Hypo	$4.2 \cdot 10^{-8}$	0.002	SHOX2

All the significant probes (FDR<0.05) for DQ analyses are included. However, only the top 15 probes are included in the DQF analysis.

Supplementary Table 2. Statistical analysis for comparing baseline, 3 month, and 6 month methylation risk score surrogates in the Dasatinib and Quercetin study.

Supplementary Table 3. Statistical analysis for comparing baseline and 6-month methylation risk score surrogates in the Dasatinib, Quercetin, and Fisetin study.